

## **Chapter 1**

# **Enhancement of digital photographs using color transfer techniques**

FRANÇOIS PITIÉ

Electronic & Electrical Department  
Trinity College Dublin  
Ireland  
Email: fpitie@mee.tcd.ie

ANIL KOKARAM

Electronic & Electrical Department  
Trinity College Dublin  
Ireland  
Email: anil.kokaram@tcd.ie

ROZENN DAHYOT

Computer Science Department  
Trinity College Dublin  
Ireland  
Email: rozenn.dahyot@tcd.ie

---

## 1.1 Introduction

Colour is an essential aspect of a picture which conveys to the viewer many emotions and symbolic meanings. Adjusting the colour grade of pictures is therefore an important step in professional photography. This process is part of the larger activity of grading in which the colour and grain aspects of the photographic material are digitally manipulated. The term colour grading will be used specifically to refer to the matching of colour. Colour grading is a delicate task since the slightest of colour variations can alter the mood of a picture. For instance, changing the white point of a picture can make a picture look warmer or more metallic. Increasing the contrast can give a sharper aspect to the picture. Colour grading is an even more critical step in movie post-production. Like with photographic stills, it gives the movie a unique artistic signature. For instance the movie *Amélie* (2002) has a look of its own. Bright colours, deep black levels and saturated colours all contribute to create an artificial expressionistic world. The main problem of grading a movie is to adjust the colour consistently across all the shots, even though the movie has been edited with heterogeneous video material. Shots taken at different times under natural light can have a substantially different *feel* due to even slight changes in lighting. Currently in the industry, colour balancing (as it is called) is achieved by experienced artists who use very expensive edit hardware and software to manually match the colour between frames by tuning parameters. Typical tuning operations comprise adjusting the exposure, brightness and contrast, calibrating the white point or finding a colour mapping curve for the luminance levels and the three colour channels. For instance, in an effort to balance the contrast of the red colour, the digital samples in the red channel in one frame may be multiplied by some gain factor and the output image viewed and compared to the colour of some other (a target) frame. The gain is then adjusted if the match in colour is not quite right. The amount of adjustment and whether it is an increase or decrease depends crucially on the experience of the artist. This is a delicate task since the change in lighting conditions induces a very complex change of illumination. It would be therefore beneficial to automate this task in some way.

The scope of colour grading goes beyond the sole photographic and post-production activities. In digital restoration [1], the goal is to recover the original colours of paintings that have been faded by smoke or dust. The process can also be used for colour image equalisation for scientific data visualisation [2, 3]. Also, the specialised activities of high dynamic range tone mapping [4, 5], as well as the grayscale to colour [6] and colour to grayscale processes [7, 8], could be considered as special instances of colour grading.

**How does colour grading work?** The colour grading workflow typically begins with grading the tone of the entire picture and then proceeds to local colour correction where specific areas of the image are isolated for dedicated colour grading. When dealing with image sequences, a tracking operation is then necessary to keep local colour corrections accurate across the whole shot. This chapter presents techniques which

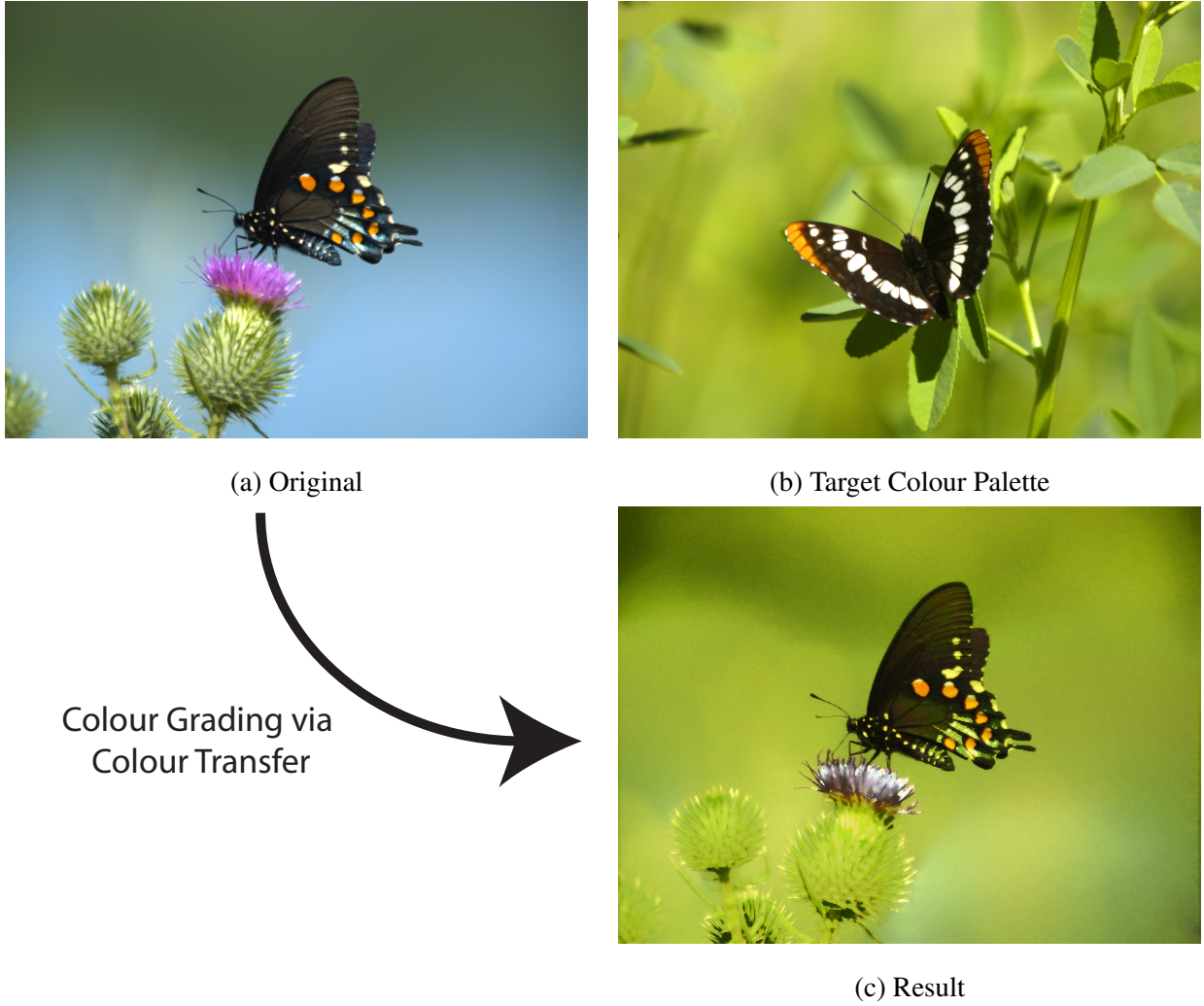


Figure 1.1: Colour transfer example. A colour mapping is applied on the original picture (a) to match the palette of an example (b) provided by the user.

aim at facilitating the choice of the colour mappings. These techniques belong to the class of example-based **colour transfer** methods. The idea, first formulated by Reinhard *et al.*[9], has raised a lot of interest recently [10, 11, 12, 13]. Figure 1.1 illustrates this with an example. The original picture (a) is transformed so that its colours match the palette of the image (b), regardless of the content of the pictures. Consider the two pictures as two sets of three dimensional colour pixels. A way of treating the re-colouring problem would be to find a one-to-one colour mapping that is applied for every pixel in the original image. For example in Figure 1.1, every blue pixel is re-coloured in green. The new picture is identical in every aspect to the original picture, except that the picture now exhibits the same colour statistics, or palette, as the target picture.

Other colour grading workflows could also be considered. Another way of treating the problem would be to re-colour the picture in compliance with the actual 3D illumination structure of the scene. This kind of

idea has been explored by Shen and Xin [14] with the aim of producing realistic recolouring under different illuminant. The method, derived from a dichromatic reflection model for the 3D objects, is however limited in practice by the difficulty of retrieving the necessary underlying 3D information from real photographic material. Another approach to colour grading is to combine the color transfer mapping with the texture information. In particular it is worth mentioning the colourisation of grayscale images by Welsh *et al.*[6] which draws from the recent success of non-parametric texture synthesis and transfer by Efros [15, 16] and Hertzmann [17]. The proposal is to replace the colour of each pixel in the original image with the colour of the best matching pixel in the example image. The best matching pixel is found by looking at the closest luminance image patch in the example image. The idea is that the colour mapping will be more accurate if it is guided by the content information given by the neighbouring texture. Bae *et al.*[18] have proposed a decomposition of the picture into a textured and a textureless layer followed by an application of the colour transfer separately for the textured layer of the image and the textureless layer. This chapter will however not consider the texture information directly. Instead it will focus on the sole problem of finding a colour mapping that transfers the colour statistics of a picture example back to the original picture. Note that Welsh's and Bae's techniques still manipulate this idea of transfer of statistics, except that in their case the transfer is conditioned to the texture information.

The notion of transfer of statistics encompasses an entire range of possibilities from the simple match of the mean, variances [9], covariance [10, 19] to the exact transfer of the exact distribution of the colour samples [20, 11, 13]. Thus, depending on how close the graded picture should match the colour distribution of the example image, multiple techniques could be used. As will be explained, finding a colour mapping is actually closely related to the *mass transportation* problem, which has a well established mathematical background [21, 22, 23]. This chapter aims then at conducting a comprehensive review of existing colour statistic transfer techniques under this new perspective. The review, presented in section 1.2, references existing work but also discloses new techniques that could be advantageously used.

**How to deal with content variations?** One important aspect of the colour transfer problem is the change of content between the two pictures. Consider a pair of landscape images where the sky in one picture covers a larger area than in the other. When transferring the colour from one picture to the other, the excess of sky colour may be used in parts of the scenery of the ground in the other. This is because all colour transfer algorithms are sensitive to variations in the areas of the image occupied by the same colour. They risk overstretching the colour mappings and thus producing unbelievable renderings as visible on Figure 1.2 which are very grainy. To deal with this issue a simple solution [9, 10, 14] is to manually select swatches in both pictures and thus associate colour clusters corresponding to the same content. This is tantamount to performing manual image segmentation, and is simply impractical for a large variety of images, and

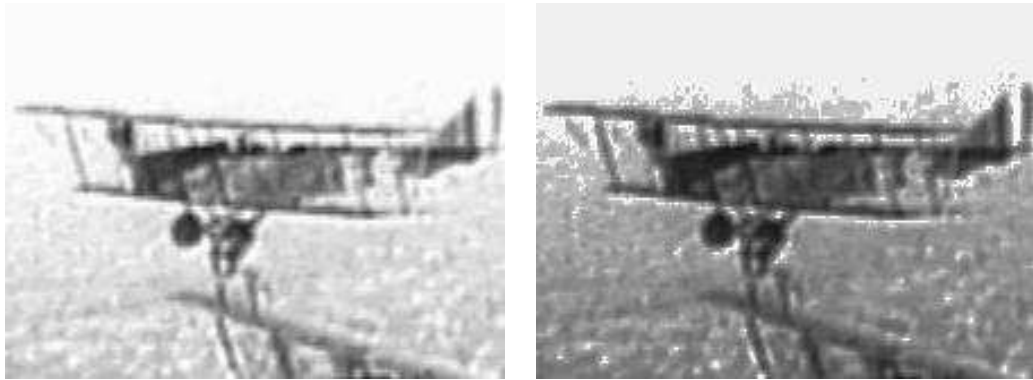


Figure 1.2: Example of Grain Induced by Colour Transfer. On the left, the original image and on the right after mapping.

certainly for sequences of images. The solution commonly adopted [11, 13] for colour transfer techniques is to simply reduce the accuracy of both distributions by smoothing the colour histograms. This simple technique avoids artefacts at the expense of an accurate transfer.

Methods that make use of the spatial information to constrain the colour mapping [6, 7, 24] can be successful but are usually computationally demanding. Another solution is to restrict the variability on the colour mapping. For example Y. Chang [25] proposes that classification of pixels of both images in a restricted set of basic colour categories, derived from psycho-physiological studies (red, blue, pink, *etc.*). The colour transfer ensures, for instance, that blue-ish pixels remain blue-ish pixels. This gives a more natural transformation. The disadvantage is that it limits the range of possible colour transfers.

The solution adopted here is to treat the grainy artefacts after the colour grading. The noise could be attenuated by employing standard colour filtering techniques [26, 27] but these would also degrade the picture itself. Instead, a dedicated post-processing is proposed which aims at protecting the original picture by preserving its original gradient field while preserving the colour transfer. This balance is done using a variational approach inspired by Poisson editing techniques [28]. Protecting the gradient of the original picture particularly protects the flat areas and more generally results in the exact reproduction of film grain/noise as in the original image.

**Organisation of the Chapter.** A review of techniques for transferring colour statistics is first presented in section 1.2. The review is accompanied with a table of comparative results. The review presents techniques to find linear mapping in section 1.3 and then non-linear mappings in section 1.4. Section 1.5 deals with the impact of the colour space. The problem of dealing with content variations and the steps of the re-graining stage are then explained in section 1.6. The chapter is concluded in section 1.7 with some examples coming from applications where colour transfer is applied.

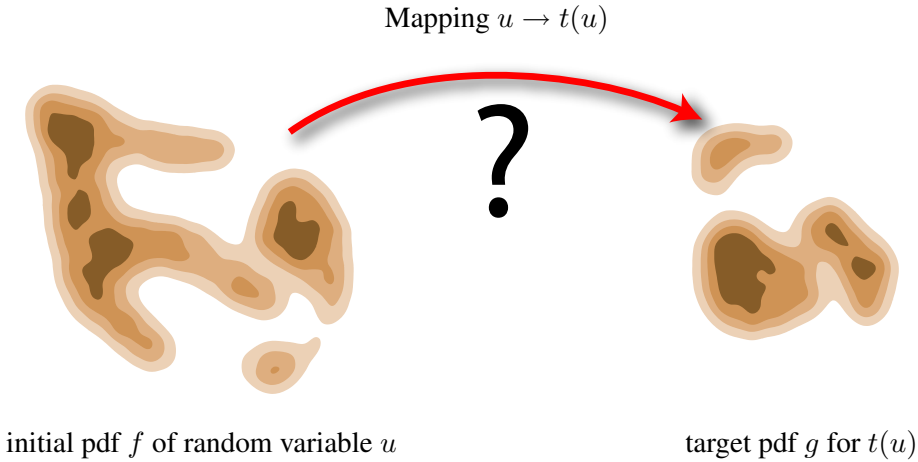


Figure 1.3: Distribution Transfer Concept. How to find a mapping that transforms the distribution on the left to the distribution on the right?

## 1.2 Colour Distribution Transfer

The notion of colour statistics can be understood by considering that an image can be represented as a set of colour samples. When working in RGB colour space, the image is represented by the set of the RGB colour samples  $(R^{(i)}, G^{(i)}, B^{(i)})_{1 \leq i \leq M}$ . In a probabilistic sense, these colour samples are realisations of a 3-dimensional colour random variable and which will be denoted as  $u$  for the original image and  $v$  for the target palette image. The colour palette of the original and target pictures correspond then to the distributions of  $u$  and  $v$ . To simplify the presentation of the problem, it is supposed here that both distributions have absolutely continuous probability density function (pdf)  $f$  and  $g$ . In practice, pdfs can only be numerically approximated. The simplest form of approximation would be colour histograms. Since only a finite number of colour samples are available, colour histograms are usually very sparse and rough. The pdfs estimation can be improved by smoothing the histograms or even better by using standard kernel density approaches. The reader is invited to read Silverman [29] for more details on density estimation. One general idea of density estimation is that the amount of smoothing controls the degree of accuracy of the pdfs. At the extreme, the pdfs can be approximated up to simple Multivariate Gaussian (MVG) distributions by estimating only the mean and the correlation matrices of  $u$  and  $v$ . Now that the notion of a colour statistic has been properly introduced, the colour transfer problem can then be defined as follows.

The problem of colour transfer is to find a  $C^1$  continuous mapping  $u \rightarrow t(u)$ , such that the new colour distribution of  $t(u)$  matches the target distribution  $g$ . This latter problem, illustrated in Figure 1.3 is also known as the *mass preserving transport problem* in the mathematical literature[21, 22, 23].

To characterise the mapping, it is worth noticing that the mapping is, in essence, a change of variables.

Thus the transfer equation can be written as:

$$f(u)du = g(v)dv \Rightarrow f(u) = g(t(u))|\det J_t(u)| \quad (1.1)$$

where  $J_t(u)$  is the Jacobian of  $t$  taken at  $u$ . Using the cumulative distribution functions  $F$  and  $G$  for  $f$  and  $g$ , the condition for the mapping to realise the transfer is derived as follows:

$$\forall u \in \mathbb{R}^N, F(u) = G(t(u)) \quad (1.2)$$

It is essential to realise here that the colour mapping corresponds to a warping of the cumulative distribution function and not of the pdf. In grayscale images [30] where  $N = 1$ , it is possible to invert the cumulative distribution function  $G$ , and the mapping has this simple form:

$$\forall u \in \mathbb{R}, t(u) = G^{-1}(F(u)) \quad (1.3)$$

where  $G^{-1}(\alpha) = \inf \{u | G(u) \geq \alpha\}$ . The mapping can then easily be solved by using discrete look-up tables. For higher dimensions, *i.e.* with colour images, the cumulative distribution function cannot be inverted since multiple solutions are possible. Thus multiple ways of finding a valid mapping can be achieved. Actually numerous different methods have been proposed and successfully applied to colour transfer. These will be presented hereafter in section 1.3 and 1.4. The problem encountered with most of them is that the geometry of the resulting mapping might not be as it was intended and it is possible that an exact transfer maps black pixels to white and white pixels to black. The resulting picture will have the colour proportions as expected, but locally the colours will have been swapped. To avoid this effect, a good solution is to further constrain the transfer problem and to ask the mapping to also minimise its displacement cost:

$$I[t] = \int_u \|t(u) - u\|^2 f(u) du \quad (1.4)$$

Finding this minimal mapping is known as the **Monge's optimal transportation problem**. Monge's problem has raised a major interest in mathematics in recent years[21, 22, 23] as it has been found to be relevant for many scientific fields like fluid mechanics. Another formulation of this problem is the **Kantorovitch's** optimal transportation problem which offers a relaxation of the one-to-one mapping constraint by allowing one colour to be mapped into multiple colours:

$$I[t] = \int_{u,v} \pi(u, v) \|v - u\|^2 dudv \quad (1.5)$$

The associations are described in  $\pi()$  which is the joint pdf between  $u$  and  $v$ . The Kantorovitch solution is related to the Monge problem since for continuous distributions, it turns out that the Kantorovitch solution coincides with the Monge solution, *i.e.* that for continuous pdfs, the best association is a one-to-one mapping:  $\pi(u, v) = \delta(t(u) - v)$ . In the rest of the chapter, the problem will be thus referred to as the Monge-Kantorovitch (MK) problem.

This chapter is not intended to be a course on the Monge-Kantorovitch problem and the reader eager to develop a better mathematical insight is invited to read a more specialised mathematical bibliography [21, 22, 23]. To understand the interest of the MK solution in colour grading, three aspects of the MK solutions will however be reported here. The first result of importance is that the MK solution always exists for continuous pdfs and is *unique*. This means that there will no room left for ambiguity. The second property is that the MK solution is consistent with orthogonal basis changes (the MK does not depend more on one component than the other). The last result, which is of interest here, is that the MK solution is the gradient of a convex function<sup>1</sup>:

$$t = \nabla \phi \quad \text{where} \quad \phi : \mathbb{R}^N \rightarrow \mathbb{R} \quad \text{is convex} \quad (1.6)$$

This might seem quite obscure at first sight, but this property is the equivalent of monotonicity for one dimensional functions in  $\mathbb{R}$ . This property is thus quite intuitive for the colour transfer problem. For instance, the brightest areas of a picture will still remain the brightest areas after mapping.

**Organisation of the Review.** The rest of this section presents techniques that have been explored in the colour grading literature, starting with the methods that consider only a linear transformation of the colour samples and then presenting the solutions that can match any colour distribution. Most of the these techniques do not solve for the Monge-Kantorovitch problem. In particular, existing literature in the domain does not propose the MK solution for the linear case but it has been introduced here and turns out to outperform other linear methods. The different techniques are compared to each other so the reader will be able to make an independent judgement. The linear methods are presented in Figure 1.6 and the non-linear methods are presented in Figure 1.7. The comparison is done for the re-colouring of the original image depicted in Figure 1.6-a to match the target palette in Figure 1.6-b. All colour transfers are done in the RGB space.

### 1.3 Linear Colour Distribution Transfer Techniques

The linear case considers the problem of finding linear mappings of the form  $t(u) = Tu + t_0$  where  $T$  is a  $N \times N$  matrix. It is not necessarily possible to find a linear mapping in the general case, but this can always be achieved when both the original distributions  $f$  and the target distributions  $g$  are multivariate Gaussian distributions (MVG)  $\mathcal{N}(\mu_u, \Sigma_u)$  and  $\mathcal{N}(\mu_v, \Sigma_v)$

$$\begin{aligned} f(u) &= \frac{1}{(2\pi)^{N/2} |\Sigma_u|^{1/2}} \exp\left(-\frac{1}{2}(u - \mu_u)^T \Sigma_u^{-1} (u - \mu_u)\right) \\ g(v) &= \frac{1}{(2\pi)^{N/2} |\Sigma_v|^{1/2}} \exp\left(-\frac{1}{2}(v - \mu_v)^T \Sigma_v^{-1} (v - \mu_v)\right) \end{aligned} \quad (1.7)$$

---

<sup>1</sup>A convex function [22]  $\phi : \mathbb{R}^N \rightarrow \mathbb{R}$  is such that  $\forall u_1, u_2 \in \mathbb{R}^N, \alpha \in [0; 1], \phi(\alpha u_1 + (1 - \alpha)u_2) \leq \alpha\phi(u_1) + (1 - \alpha)\phi(u_2)$

with  $\Sigma_u$  and  $\Sigma_v$  the covariance matrices of  $u$  and  $v$ . Note that when the distributions are not MVG, a MVG approximation can always be obtained by estimating the mean and the covariance matrices of the distributions. To have the pdf transfer condition  $g(t(u)) \propto f(u)$ , it must hold that  $(t(u) - \mu_v)^T \Sigma_v^{-1} (t(u) - \mu_v) = (u - \mu_u)^T \Sigma_f^{-1} (u - \mu_u)$ . Thus  $t$  must satisfy the following condition:

$$t(u) = T(u - \mu_u) + \mu_v \quad \text{with} \quad T^T \Sigma_v^{-1} T = \Sigma_u^{-1} \quad (1.8)$$

It turns out that there are numerous solutions for the matrix  $T$  and thus multiple ways of transferring the colour statistics.

### 1.3.1 Independent Transfer

The first method, used by Reinhard *et al.*[31] in their original paper on colour transfer, is to simply match the means and the variances of each component independently. This means that both distributions are separable, thus the covariance matrices are diagonal and  $\Sigma_u = \text{diag}(\text{var}(u_1), \dots, \text{var}(u_N))$  and  $\Sigma_v = \text{diag}(\text{var}(v_1), \dots, \text{var}(v_N))$ . It yields for the mapping that

$$T = \begin{pmatrix} \sqrt{\frac{\text{var}(v_1)}{\text{var}(u_1)}} & & 0 \\ & \ddots & \\ 0 & & \sqrt{\frac{\text{var}(v_N)}{\text{var}(u_N)}} \end{pmatrix} \quad (1.9)$$

The independence assumption is simplistic since it is rarely true for real images. The poor quality of the transfer in the results in Figure 1.6-c show that this is indeed not always the case. The solution proposed by Reinhard is to work in the decorrelated colour space  $l\alpha\beta$  of Ruderman [32]. This helps to some extent but cannot guarantee a full decorrelation between components.

### 1.3.2 Cholesky Decomposition

Since both matrices  $\Sigma_u$  and  $\Sigma_v$  are symmetric semi definite positive, a solution is to use the Cholesky decomposition of  $\Sigma_u = L_u L_u^T$  and  $\Sigma_v = L_v L_v^T$  where  $L_u$  and  $L_v$  are lower triangular matrices with strictly positive diagonal elements. This decomposition yields the following solution:

$$T = L_v L_u^{-1} \quad (1.10)$$

Note that this solution is dependent on the ordering of the colour components. Figure 1.6-d shows however some improvements on the previous method. This method is quite successful in practice but is not as reliable as the MK solution.

### 1.3.3 Principal Axes Transfer

Another popular solution [33, 19, 10, 34, 35] is to find the mapping that realigns the principal axes of  $\Sigma_v$  to that of  $\Sigma_u$ . This can be done by using the square root operator for symmetric positive semidefinite matrices. The square root matrices  $\Sigma_u^{1/2}$  and  $\Sigma_v^{1/2}$  are obtained through the spectral decomposition of  $\Sigma_u$  and  $\Sigma_v$ :

$$\Sigma_u = P_u D_u P_u^T \text{ and } \Sigma_u^{1/2} = P_u D_u^{1/2} P_u^T \quad (1.11)$$

$$\Sigma_v = P_v D_v P_v^T \text{ and } \Sigma_v^{1/2} = P_v D_v^{1/2} P_v^T \quad (1.12)$$

where  $P_u$  and  $P_v$  are orthogonal matrices and  $D_u$  and  $D_v$  the diagonal matrix containing the (positive) eigenvalues of  $\Sigma_u$  and  $\Sigma_v$ . Note that the square roots  $\Sigma_u^{1/2}$  and  $\Sigma_v^{1/2}$  are uniquely defined. These decompositions lead to the following mapping:

$$T = \Sigma_v^{1/2} \Sigma_u^{-1/2} \quad (1.13)$$

Results displayed in Figure 1.6-e show an improvement over the mapping based on the Cholesky decomposition. Note in particular that the violet colour of the grass in Figure 1.6-e is not present here. This might be due to fact that the mapping does not depend on the ordering of the colour components.

### 1.3.4 Linear Monge-Kantorovitch Solution

A better approach would be to use the Monge-Kantorovitch solution for MVG distributions. The MK solution is geometrically more intuitive than the Cholesky or the Principal Axes solution. One could be concerned that the MK solution might not be linear, but fortunately it is actually linear and it admits a simple closed form. The detailed proof of how to find the MK mapping can be found in [36]. The mainstay of the reasoning is that since the MK solution is the gradient of a convex function, the matrix  $T$  has to be symmetric definite positive, which leads to this unique solution for  $T$ :

$$T = \Sigma_u^{-1/2} \left( \Sigma_u^{1/2} \Sigma_v \Sigma_u^{1/2} \right)^{1/2} \Sigma_u^{-1/2} \quad (1.14)$$

The corresponding results in Figure 1.6-f are convincing. The results are slightly better than the ones of the Principal Axes method. For instance a pink trace on the grass in front of the house is visible in (e) but not in (f). The MK solution is thus interesting as it provides an intuitive and probably better mapping for a similar computational complexity to the popular methods.

## 1.4 Non-Linear Colour Distribution Transfer Techniques

### 1.4.1 Independent Transfer

Extending the solutions for MVG to any distribution is sadly more complicated. The approach used at the moment in professional colour grading tools is to extend the pdf transfer to higher dimensions by performing

the 1D non-linear pdf matching separately for each channel [37]. Like in the linear case, this is only exact if both distributions are separable, *i.e.* if the joint distribution is the product of its marginals:

$$f(u_1, u_2, \dots, u_N) = f(u_1)f(u_2)\cdots f(u_N) \quad (1.15)$$

This is however not realistic in most situations. The result displayed in Figure 1.7-c reflects this.

### 1.4.2 Composition Transfer

This method, that has been applied to the colour transfer problem by Neumann [11], builds on the fact that the correlated variables  $u_1, \dots, u_N$  can be recombined into the following independent variables  $u'_1, u'_2, \dots, u'_N$ :

$$u'_1 \sim f(u_1) \quad u'_2 \sim f(u_2|u_1) \quad \dots \quad u'_N \sim f(u_N|u_1, \dots, u_{N-1}) \quad (1.16)$$

The independence becomes apparent from the following conditional decomposition:

$$f(u_1, u_2, \dots, u_N) = f(u_1)f(u_2|u_1)\cdots f(u_N|u_1, \dots, u_{N-1}) \quad (1.17)$$

Since these conditional variables are independent, it is possible to use 1D pdf transfers separately for each of the conditional variables. The final mapping is then composed as follows:

$$t(u_1, \dots, u_N) = (t_1(u_1), t_2(u_2|u_1), \dots, t_N(u_N|u_1, \dots, u_{N-1})) \quad (1.18)$$

and each 1D mapping  $t_1, \dots, t_N$  is found by using the corresponding pdf transfer:

$$\begin{aligned} t_1(u_1) : f(u_1) &\Rightarrow g(v_1) \\ t_2(u_2|u_1) : f(u_2|u_1) &\Rightarrow g(v_2|v_1) \\ &\vdots \\ t_N(u_N|u_1, \dots, u_{N-1}) : f(u_N|u_1, \dots, u_{N-1}) &\Rightarrow g(v_N|v_1, \dots, v_{N-1}) \end{aligned} \quad (1.19)$$

This technique suffers from two main problems. Firstly the mapping itself depends heavily on the order in which the variables are conditioned to each other. For instance matching  $f(u_1)$  and then  $f(u_2|u_1)$  results in a different mapping than mapping  $f(u_2)$  and then  $f(u_1|u_2)$ . The second issue is that even for large pictures, the estimation of the conditionals marginals like  $f(u_N|u_1, \dots, u_{N-1})$  is based on only a very small number of colour samples since only a few pixels will have exactly the same colour. This means in practice for a RGB colour grading, that if the transfer of the first red component is accurate, the transfer of last blue component is however poor. This is reflect in Figure 1.7-d where the blue gain has been overestimated. The situation can be improved by using some proper density estimation scheme [29] which mainly implies smoothing the original 3D histogram. Note that smoothing the pdfs is a delicate operation that requires some computational time for large colour histograms.

### 1.4.3 The Discrete Kantorovitch Solution

As with the linear case, the Monge-Kantorovitch solution seems then to be more appropriate here. Numerical solutions exist for  $N$ -dimensional variables, but they involve heavy computational loads as they require the use of an iterative partial differential equations solver in the  $N$ -dimensional distribution [21]. However, to reduce the computational complexity, it is possible to segment the actual pdf to a smaller number of colours. Since the pdfs are now discretised, it might not be possible to find a one-to-one mapping that transfer one pdf exactly to another. Instead, the one-to-one mapping assumption is relaxed and it is allowed for one histogram bin to be mapped onto multiple bins. The problem is then to find the flow  $\pi()$  (joint distribution) that minimises the overall transportation cost:

$$\hat{\pi} = \inf_{\pi} \sum_{i,j} \pi(u_i, v_j) |u_i - v_j|^2 \quad (1.20)$$

with  $\forall j, \sum_i \pi(u_i, v_j) = g(u_j) \quad \forall i, \sum_j \pi(u_i, v_j) = f(u_i)$ . Note that this formulation of the transportation problem has been introduced in the computer vision community by Rubner under the name of Earth Mover Distance [38]. The discretised problem can be numerically solved by linear programming using the Simplex algorithm [39]. Several specialised algorithms for solving the transport problem also exist, notably the *northwest corner* method and the *Vogels approximation* [40]. Since a colour can be mapped into multiple colours, the issue is now of deciding which colour to assign to a particular pixel. Morovic proposes to decide for each pixel on a random basis. This process is, in a essence, similar to a randomised dithering.

One remarkable result of the MK theory is that, in the continuous case, the kantorovich solution is actually Monge's one-to-one mapping. This simply means that increasing the number of bins will reduce the dithering and gives a better approximate of Monge's colour mapping. The problem is that the Simplex algorithm is quite slow and becomes intractable when dealing with large histograms. The result in Figure 1.7-e has been obtained for a colour histogram of 300 colour bins. Despite these limitations, the method still produces visibly better results than the previously presented methods.

### 1.4.4 Transfer via the Radon Transform

Recently, Pitié *et al.* [41] have proposed another solution to the distribution transfer problem which is based on the iterative use of 1D transfers for various directions in the  $N$  dimensional space. The idea is to break down the problem into a succession of 1-Dimensional distribution transfer problems. Consider the use of the  $N$ -dimensional Radon Transform. It is widely acknowledged that via the Radon Transform, any  $N$ -dimensional function can be uniquely described as a series of projections onto 1-dimensional axes [42] (see Figure 1.4). In this case, the function considered is a  $N$ -dimensional pdf, hence the Radon Transform projections result in a series of 1-dimensional marginal pdfs from which can be derived the corresponding 1D pdf

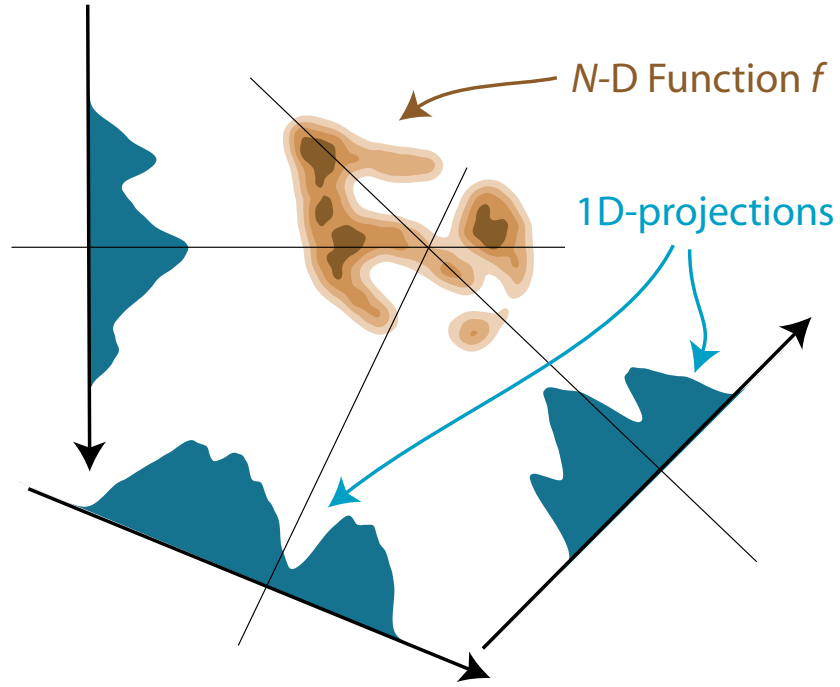


Figure 1.4:  $N$ -dimensional Radon transform of a distribution's pdf. The pdf is projected onto every possible axis. Each projection corresponds to a 1D marginal of the distribution. The ensemble of all projections uniquely describes the distribution.

transfers along these axes. Intuitively then, operations on the  $N$ -dimensional pdf should be possible through applying the 1D pdf transfer along these axes. Consider that after some sequence of such manipulations, all 1-dimensional marginals match the corresponding marginals of the target distribution. It then follows that, by nature of the Radon Transform, the transformed  $f$ , corresponding to the transformed 1-dimensional marginals, now matches  $g$ .

The operation applied to the projected marginal distributions is thus similar to that used in 1-dimension. Denote a particular axis by its vector direction  $e \in \mathbb{R}^N$ . The projection of both pdfs  $f$  and  $g$  onto the axis  $e$  results in two 1-dimensional marginal pdfs  $f_e$  and  $g_e$ . Using the 1-dimensional pdf transfer mapping of the equation (1.3) yields a 1-dimensional mapping  $t_e$  along this axis:

$$\forall u \in \mathbb{R}, t_e(u) = G_e^{-1}(F_e(u)) \quad (1.21)$$

For a  $N$ -dimensional sample  $u = [u_1, \dots, u_N]^T$ , the projection of the sample on the axis is given by the scalar product  $e^T u = \sum_i e_i u_i$ , and the corresponding displacement along the axis is

$$u \rightarrow u + \delta \quad \text{with} \quad \delta = (t_e(e^T u) - e^T u) e \quad (1.22)$$

After transformation, the projection  $f'_e$  of the new distribution  $f'$  is now identical to  $g_e$ . The manipulation is explained in figure 1.5. Considering that the operation can be done independently on orthogonal axes, the

Table 1.1: Optimised rotations for  $N = 3$ 

No.	1			2			3		
x	1	0	0	0.333333	0.666667	0.666667	0.577350	0.211297	0.788682
y	0	1	0	0.666667	0.333333	-0.666667	-0.577350	0.788668	0.211352
z	0	0	1	-0.666667	0.666667	-0.333333	0.577350	0.577370	-0.577330
No.	4			5			6		
x	0.577350	0.408273	0.707092	0.332572	0.910758	0.244778	0.243799	0.910726	0.333376
y	-0.577350	-0.408224	0.707121	-0.910887	0.242977	0.333536	0.910699	-0.333174	0.244177
z	0.577350	-0.816497	0	-0.244295	0.333890	-0.910405	-0.333450	-0.244075	0.910625
No.	7			8			9		
x	-0.109199	0.810241	0.575834	0.759262	0.649435	-0.041906	0.862298	0.503331	-0.055679
y	0.645399	0.498377	-0.578862	0.143443	-0.104197	0.984158	-0.490221	0.802113	-0.341026
z	0.756000	-0.308432	0.577351	0.634780	-0.753245	-0.172269	-0.126988	0.321361	0.938404
No.	10			11			12		
x	0.982488	0.149181	0.111631	0.687077	-0.577557	-0.440855	0.463791	0.822404	0.329470
y	0.186103	-0.756525	-0.626926	0.592440	0.796586	-0.120272	0.030607	-0.386537	0.921766
z	-0.009074	0.636722	-0.771040	-0.420643	0.178544	-0.889484	-0.885416	0.417422	0.204444

proposed manipulation consists in choosing an orthogonal basis  $R = (e_1, \dots, e_N)$  and then applying the following mapping:

$$u \rightarrow u + R \begin{pmatrix} t_1(e_1^T u) - e_1^T u \\ \vdots \\ t_N(e_N^T u) - e_N^T u \end{pmatrix} \quad (1.23)$$

where  $t_i$  is the 1-dimensional pdf transfer mapping for the axis  $e_i$ .

The idea is that iterating this manipulation over different axes will result in a sequence of distributions  $f^{(k)}$  that hopefully converges to the target distribution  $g$ . The overall algorithm will be referred to as the **Iterative Distribution Transfer (IDT)** algorithm. The outline of the algorithm is displayed on page 15.

A theoretical and numerical study of the method are developed in more depth in [41]. The experimental study strongly suggests that convergence occurs for any distribution. The study also considers the problem of finding a sequence of axes that maximises the convergence speed of the algorithm. The sequence of axes is designed to minimise the correlation between the directions. A table of these directions for the case  $N = 3$  is report in table 1.1.

As in the composition transfer case, the manipulations are based on the use of 1D marginals. The difference is that the marginals are not based on conditional probabilities. This means that the operation is independent of the channel ordering. Also, the estimation of the marginals does not suffer from the data sparseness and the  $N$ -dimensional pdf does not need to be smoothed. In contrast with the discrete Kantorovitch method, the method is treated with one-to-one mapping all along, thus no dithering post-process is necessary. Figure 1.7-f shows that the results are quite similar to the discrete Kantorovitch solution.

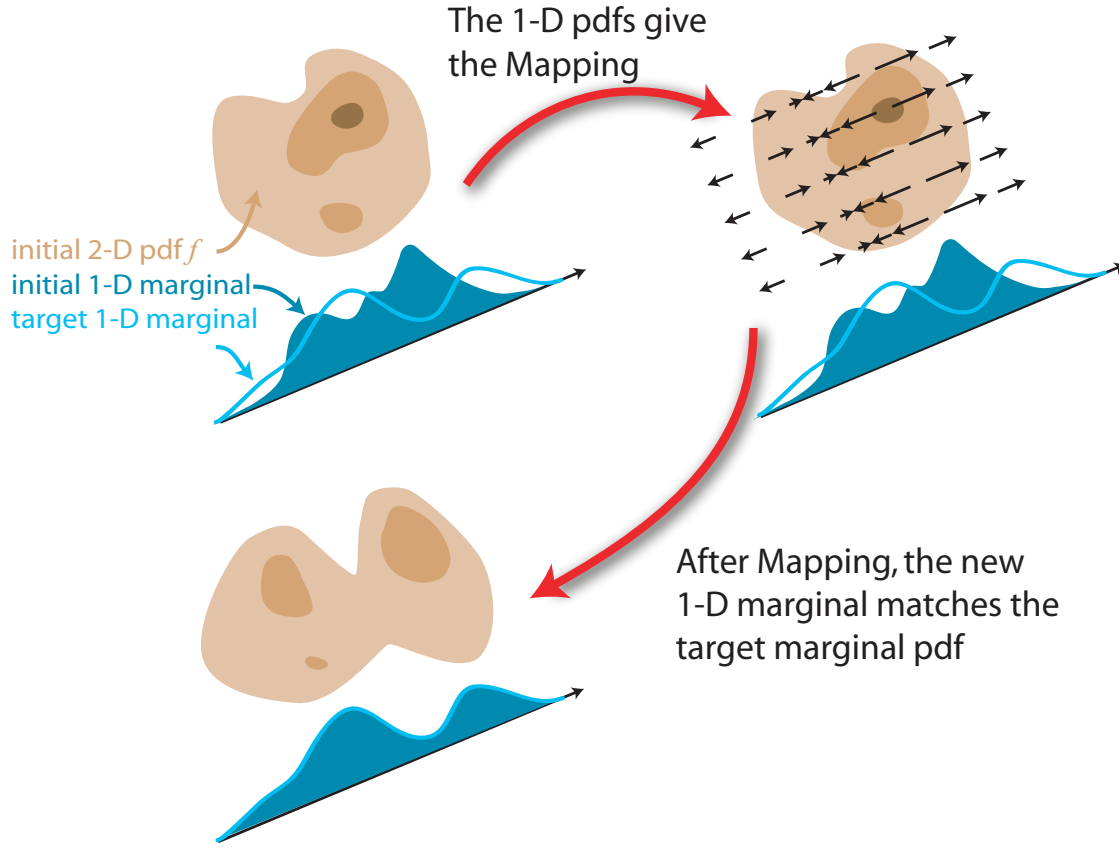


Figure 1.5: Illustration of the data manipulation, based on the 1-dimensional pdf transfer on one axis.

---

#### Algorithm 1 Iterative Distribution Transfer using the Radon Transform

---

1: **Initialisation** of the data set source  $u$ , set the displacement  $\delta$  to zero:

$$k \leftarrow 0, \delta^{(0)} \leftarrow 0$$

2: **repeat**

3:   take a rotation matrix  $R = [e_1, \dots, e_N]$

4:   for every rotated axis  $i$  of the rotation, get the projections  $f_i^{(k)}$  of  $\{u + u^{(k)}\}$  and  $g_i$  of  $\{v\}$

5:   for every rotation axis  $i$ , find the 1D transformation  $t_i$  that matches the marginals  $f_i$  into  $g_i$

6:   update the displacement  $\delta$ :

$$\delta^{(k+1)} = \delta^{(k)} + R \begin{pmatrix} t_1(e_1^T(u + \delta^{(k)}) - e_1^T(u + \delta^{(k)})) \\ \vdots \\ t_N(e_1^T(u + \delta^{(k)}) - e_N^T(u + \delta^{(k)})) \end{pmatrix}$$

7:    $k \leftarrow k + 1$

8: **until** convergence on all marginals for every possible rotation

9: The final one-to-one mapping  $T$  is given by:  $\forall j, u_j \mapsto t(u_j) = u_j + \delta_j^{(\infty)}$

---



(a) Original



(b) Target palette



(c) Separable linear transfer



(d) Cholesky based transfer



(e) Principal Axes transfer



(f) Linear Monge-Kantorovitch transfer

Figure 1.6: Results for linear techniques. All transfers are done in the RGB colour space.



(a) Original



(b) Target palette



(c) Separable transfer



(d) Composition transfer



(e) Discrete Kantorovitch



(f) IDT

Figure 1.7: Results for different scenarios

## 1.5 What Colour Space to Choose?

If a method can exactly transfer the complete colour statistics, then this method will work regardless of the chosen colour space. Thus, in that respect, the colour space is not important to transfer the colour ‘feel’ of an image. The colour space has however an influence on the geometrical form of the colour mapping. In the MK formulation for instance, the cost of transportation is related to the colour difference, which depends on the chosen colour space. Thus uniform colour spaces like YUV, or better CIELAB and CIELUV, are preferable to the basic RGB to obtain coherent colour mappings. Comparative results for RGB, YUV, CIE XYZ, CIELAB and CIELUV are displayed in Figure 1.8 for the linear MK solution and in Figure 1.9 for the proposed IDT method. Differences might be difficult to see on printed images, but these are very significant when displayed on a big screen, especially if they are images in a sequence which is played back. The CIELAB colour space overall offers better renderings, for the linear and the non-linear case. This is because it is designed to measure the difference between colours under different illuminants.

## 1.6 Reducing Grain Noise Artefacts

Figure 1.10 and Figure 1.11 show that mapping the colours of the picture might produce some grain artefacts. When the content differs, or when the dynamic ranges of both pictures are too different, the resulting mapping function can be stretched on some parts (see figure 1.10-e), and thus enhances the noise level (see figure 1.10-c). This can be understood by taking the simple example of a linear transformation  $t$  of the original picture:  $t(u) = a u + b$ . The overall variance of the resulting picture is changed to  $\text{var}\{t(u)\} = a^2 \text{var}\{u\}$ . This means that a greater stretching ( $a > 1$ ) produces more noise.

The problem is that it is impossible to say a priori if the large difference in the distributions is due to a drastic colour mapping, which is always possible, or due to a content variation. The difficulty of differentiating these cases is the Achilles’ heel of example based colour transfer techniques. Since any distribution can map any other distribution, it is impossible to impose any prior on the distributions. This issue remains an open problem but a few ad hoc solutions can help here. Solutions in the literature [13, 11] have been proposed to use a pre-processing smoothing operation on the pdfs. The motivation for these solutions, exposed hereafter, is to reduce the over-stretching of the mapping. This chapter also proposes a post-processing method to protect the original picture gradient and thus reduce the amount of artefacts.

### 1.6.1 Reducing the Stretching by Pre-Processing the Distributions

One origin of the artefacts is that the target pdf is usually only a rough estimate of what the true palette should be. This means that using very accurate pdf approximations might lead to erroneous transfers. In that



(a) target colour palette



(b) RGB



(c) YUV



(d) XYZ



(e) CIELAB



(f) CIELUV

Figure 1.8: Colour-Space. Results of the Linear Monge-Kantorovitch transfer for different colour spaces.



(a) target colour palette



(b) RGB



(c) YUV



(d) XYZ



(e) CIELAB



(f) CIELUV

Figure 1.9: Colour-Space. Results of the IDT transfer for different colour spaces.

sense, using simple MVG approximations is always a safer solution. Also an advantage of linear mappings is that they have a constant stretching  $|t'(u)| = |\Sigma_v|^{1/2}/|\Sigma_u|^{1/2}$  over the colour distribution. The colour deformation is thus also constant over the whole image and the artefacts are uniformly distributed over the picture.

Non-linear mappings have however to be used when dealing with complex illuminations. In order to avoid unnecessary finesse in the approximations, what is desired is a mechanism that controls the level of approximation. This control can be achieved by smoothing the colour histograms by a variable amount. The smoothing can be done by employing a kernel filter  $K$  with bandwidth  $h$ . For instance, one can use the Epanechnikov kernel, which is the function  $K_h(u) = (3/4)(1 - \|u/h\|^2)$  for  $\|u/h\| < 1$  and zero for  $\|u/h\|$  outside that range. The smoothness of the pdf is then controlled by the bandwidth parameter  $h$ . Decreasing  $h$  increases the detail level of the pdf.

Smoothing the pdf reduces distortions that are due to fine disparities, but does not specifically address the problem of change of colour proportions. Consider the example, previously discussed, where the sky in one picture covers a larger area than in the other. The peak in the pdf corresponding to the blue colour is at the same location in both pdfs, but the mass of this peak is then different. Smoothing the pdf solves this problem only partially. A solution used by Pitié [13] and Neumann [11] is to reduce the relative size of each peak in the pdfs. In this way, the variations in colour proportions is limited. Combining both smoothing and this dominant colour correction idea results in the following ad hoc smoothing operation on the pdf:

$$\tilde{f}(u) = (K_h * f(u) + \epsilon)^{(1/p)} \quad (1.24)$$

where the exponent  $p > 1$  controls the relative size of the pdf peaks and  $\epsilon$  avoids problems when  $f(u) = 0$ . When working with 1D marginals, like the IDT algorithm does, the smoothing can be applied to the 1D marginals and not the original ND pdf.

Bear in mind however that this smoothing operation should not be used if the target distribution is actually the one desired, since in that case the resulting mapping would then be erroneous. The best solution is to leave most of the correction process to the regrain post-processing which is explained in the following section.

## 1.6.2 Reducing the Artefacts by a-la Poisson Image Post-Processing

A solution to reduce the grain is to run a post-processing algorithm that forces the noise level to remain the same. The idea presented by Pitié *et al.*[41] is to adjust the gradient field of the resulting picture so that it matches the gradient field of the original picture. If the gradient fields of both pictures are similar, the noise level will be the same. Matching the gradient of a picture has been addressed in different computer vision applications like high dynamic range compression [4]; the value of this idea has been thoroughly

demonstrated by Pérez *et al.* in [28]. Manipulating the image gradient can be efficiently done by using a variational approach. The problem here is slightly different, since re-colouring also implies changing the contrast levels. Thus the new gradient field should only loosely match the original gradient field.

Denote  $I(x, y)$  the 3-dimensional original colour picture. To simplify the discussion, coordinates are omitted in the expressions and  $I, J, \psi, \phi$ , etc. actually refer to  $I(x, y), J(x, y), \psi(x, y)$  and  $\phi(x, y)$ . Let  $t : I \rightarrow t(I)$  be the colour transformation. The problem is to find a modified image  $J$  of the mapped picture  $t(I)$  that minimises on the whole picture range  $\Omega$

$$\min_J \iint_{\Omega} \phi \cdot \|\nabla J - \nabla I\|^2 + \psi \cdot \|J - t(I)\|^2 dx dy \quad (1.25)$$

with Neumann boundaries condition  $\nabla J|_{\partial\Omega} = \nabla I|_{\partial\Omega}$  so that the gradient of  $J$  matches with the gradient of  $I$  at the picture border  $\partial\Omega$ . The term  $\|\nabla J - \nabla I\|^2$  forces the image gradient to be preserved. The term  $\|J - t(I)\|^2$  ensures that the colours remain close to the target picture and thus protects the contrast changes. Without  $\|J - t(I)\|^2$ , a solution of equation (1.25) will be actually the original picture  $I$ .

The weight fields  $\phi(x, y)$  and  $\psi(x, y)$  affect the importance of both terms. Many choices are possible for  $\phi$  and  $\psi$ , and the following study could be easily be changed, depending on the specifications of the problem.

The weight field  $\phi(x, y)$  has been here chosen to emphasise that only flat areas have to remain flat but that gradient can change at object borders:

$$\phi = \frac{30}{1 + 10 \|\nabla I\|} \quad (1.26)$$

The weight field  $\psi(x, y)$  accounts for the possible stretching of the transformation  $t$ . Where  $\nabla t$  is big, the grain becomes more visible:

$$\psi = \begin{cases} 2 / (1 + \|(\nabla t)(I)\|) & \text{if } \|\nabla I\| > 5 \\ \|\nabla I\| / 5 & \text{if } \|\nabla I\| \leq 5 \end{cases} \quad (1.27)$$

where  $(\nabla t)(I)$  is the gradient of  $t$  for the colour  $I$  and thus refers to the colour stretching. The case  $\|\nabla I\| \leq 5$  is necessary to re-enforce that flat areas remains flat. While the gradient of  $t$  is easy to estimate for grayscale pictures, it might be more difficult to obtain for colour mappings. The field can then be changed into:

$$\psi(x, y) = \begin{cases} 1 & \text{if } \|\nabla I\| > 5 \\ \|\nabla I\| / 5 & \text{if } \|\nabla I\| \leq 5 \end{cases} \quad (1.28)$$

**Numerical Solution.** The minimisation problem in equation (1.25) can be solved using the variational principle which states that the integral must satisfy the Euler-Lagrange equation:

$$\frac{\partial F}{\partial J} - \frac{d}{dx} \frac{\partial F}{\partial J_x} - \frac{d}{dy} \frac{\partial F}{\partial J_y} = 0 \quad (1.29)$$

where

$$F(J, \nabla J) = \phi \cdot ||\nabla J - \nabla I||^2 + \psi \cdot ||J - t(I)||^2 \quad (1.30)$$

from which the following can be derived:

$$\phi \cdot J - \operatorname{div}(\psi \cdot \nabla J) = \phi \cdot t(I) - \operatorname{div}(\psi \cdot \nabla I) \quad (1.31)$$

This is an elliptic partial differential equation. The expression  $\operatorname{div}(\psi \cdot \nabla I)$  at pixel  $\mathbf{x} = (x, y)$  can be approximated using standard finite differences [43] by:

$$\operatorname{div}(\psi \cdot \nabla I)(\mathbf{x}) \approx \sum_{\mathbf{x}_n \in \mathcal{N}_{\mathbf{x}}} \frac{\psi_{\mathbf{x}_n} + \psi_{\mathbf{x}}}{2} (I_{\mathbf{x}_n} - I_{\mathbf{x}}) \quad (1.32)$$

where  $\mathcal{N}_{\mathbf{x}}$  corresponds to the four neighbouring pixels of  $\mathbf{x}$ . Using this in equation (1.31) yields a linear system as follows:

$$\begin{aligned} a_1(x, y)J(x, y - 1) + a_2(x, y)J(x, y + 1) + a_3(x, y)J(x - 1, y) \\ + a_4(x, y)J(x + 1, y) + a_5(x, y)J(x, y) = a_6(x, y) \end{aligned} \quad (1.33)$$

with

$$a_1(x, y) = -\frac{\psi(x, y - 1) + \psi(x, y)}{2} \quad (1.34)$$

$$a_2(x, y) = -\frac{\psi(x, y + 1) + \psi(x, y)}{2} \quad (1.35)$$

$$a_3(x, y) = -\frac{\psi(x - 1, y) + \psi(x, y)}{2} \quad (1.36)$$

$$a_4(x, y) = -\frac{\psi(x + 1, y) + \psi(x, y)}{2} \quad (1.37)$$

$$a_5(x, y) = \frac{1}{2} (4\psi(x, y) + \psi(x, y - 1) + \psi(x, y + 1) + \psi(x - 1, y) + \psi(x + 1, y)) + \phi(x, y) \quad (1.38)$$

$$\begin{aligned} a_6(x, y) = & \frac{1}{2} \left( (\psi(x, y) + \psi(x, y - 1))(I(x, y - 1) - I(x, y)) \right. \\ & + (\psi(x, y) + \psi(x, y + 1))(I(x, y + 1) - I(x, y)) \\ & + (\psi(x, y) + \psi(x - 1, y))(I(x - 1, y) - I(x, y)) \\ & \left. + (\psi(x, y) + \psi(x + 1, y))(I(x + 1, y) - I(x, y)) \right) \phi(x, y) I(x, y) \end{aligned} \quad (1.39)$$

The system can be solved by standard iterative methods like SOR or Gauss-Seidel with multigrid approach. Implementations of these numerical solvers are widely available and one can refer for instance to Numerical Recipes [44]. The main step of these methods is to solve iteratively for  $J(x, y)$ . Note that  $J(x, y)$  and  $a_i(x, y)$  are of dimension 3, but that each colour component can be treated independently. For instance,

the iteration for the red component field is of the form

$$\begin{aligned} J_R^{(k+1)}(x, y) = & \frac{1}{a_5^R(x, y)} \left( a_5^R(x, y) - a_1^R(x, y)J_R^{(k)}(x, y-1) - a_2^R(x, y)J_R^{(k)}(x, y+1) \right. \\ & \left. - a_3^R(x, y)J_R^{(k)}(x-1, y) - a_4^R(x, y)J_R^{(k)}(x+1, y) \right) \end{aligned} \quad (1.40)$$

where  $J_R^{(k)}(x, y)$  is the result in the red component at the  $k^{th}$  iteration.

**Re-graining Results.** The overall method takes less than a second per image at PAL resolution ( $720 \times 576$ ) on a 2GHz machine using a commercial implementation of the method. Figure 1.10-e and Figure 1.11-c show the efficiency of the method. In Figure 1.10-e, the top of the original frame is clamped thus the loss of grain texture. Note that the re-graining method is well designed for this kind of situation where the mapping is actually correct and artefacts only come from the discrete nature of the image. The case of Figure 1.11 is more difficult since the target colour pdf can only be a crude approximation of what is desired. However the re-graining tool is quite successful at recovering the original gradient information in the resulting image (c).

## 1.7 Application Results

The colour transfer techniques are tested here for some colour grading applications. Considering the advantages of the MK solution for the linear case and of the IDT method for the non-linear case, only these methods will be used in the following examples. Also, the IDT will be systematically used in conjunction with the re-graining process. The algorithms work in the CIELAB colour space.

**Matching Lighting Conditions.** Matching lighting conditions is illustrated in Figure 1.12 in two typical situations. On the left column, the colour properties of the sunset (a2) are used to synthesise the ‘evening’ scene (a1) depicted at sunset (a3). This kind of grading is frequent when shooting a movie at sunset since the light is changing quickly. To be able to cope with the non-linearity of the contrast change, the colour transfer is performed by using IDT. On the second column, the colour grading corrects another classical change of lighting conditions due to passing clouds. Even when using the grain artefact reducer, an unavoidable limitation of colour grading is the clipping of the colour data: saturated areas cannot be retrieved (for instance the sky on the golf image cannot be recovered). A general rule is to match pictures from higher to lower range dynamics.

**Movie Restoration.** Figure 1.13 displays examples of colour restoration of faded movies. The idea is similar to colour grading, *i.e.* it is to enhance the colour and match a desired atmosphere. The target pictures used for recreating the atmosphere are on the left column. The corresponding results are presented on the



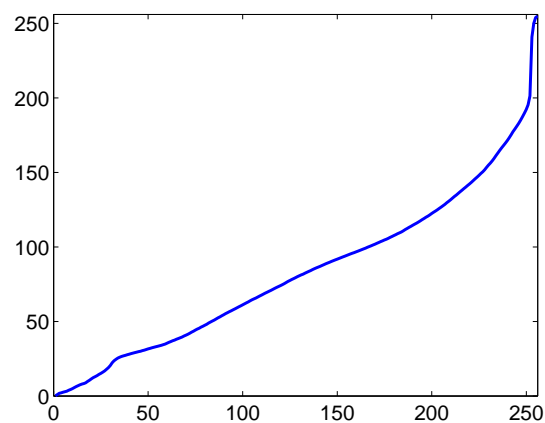
(a) original



(b) target palette



(c) recoloured



(d) mapping



(e) re-grained

Figure 1.10: Result of grain reducing. The two consecutive archive frames (a) and (b) suffer from extreme brightness variation (this artefact is known as flicker [45]). The corresponding mapping transformation (e) is overstretched, which results in an increased level of noise in the mapped original frame (c). The proposed grain artefact reducer is able to reproduce the noise level of the original picture. The top of the original picture is saturated and cannot be retrieved but the algorithm succeeds in preserving the soft gradient.



(a) original



(b) after IDT colour transfer



(c) after re-graining

Figure 1.11: Artefact grain reducing for colour picture. See how the details of the picture are preserved, while the spurious graininess in the sky is washed out.

right. Note that the Linear MK method can be enough to enhance properly the faded colour palette. The IDT can however recreate a wider variety of grades than the linear MK method. For instance the IDT can produce both images (d) and (e) whereas the linear MK solution will fail at reproducing the strong contrasts of (e). To realise (e), the smoothing process (see section 1.6.1) has been used before starting the IDT.

**Photography.** Figure 1.14 and 1.7 present two examples of colour grading for photography. Because images are not played back in photography, the consistency is not as critical as it is in movie post-production. If the IDT method provides the closest colour feel to the target picture, the linear MK transformation can sometimes satisfy aesthetically the artist and serves as a starting point for further editing.

**Colour Equalisation.** It is possible with the IDT algorithm to perform true colour equalisation by choosing the uniform distribution as a target. As illustrated in Figure 1.7, the equalisation process puts the whole colour spectrum in the image. Note that even though the mapping is extremely stretched, the smoothness of the picture is still preserved by the re-graining process.

## 1.8 Parting Remarks

This chapter has presented a review of colour transfer techniques that are based on one-to-one colour mappings. It has also established that these methods have a common mathematical background which is the mass transportation theory and that a good way of dealing with the problem is to use the Monge-Kantorovitch mappings. Monge-Kantorovitch mappings have intuitive geometrical properties and turn out to be robust when used in real applications. Thus finding mappings that transfer colour statistics is now a well understood problem. The algorithms that have been proposed here, *i.e.* the linear MK solution and the non-linear IDT method, have already been implemented in industrial applications and are currently used by artists. Grain artefacts resulting from the mapping correction have also been addressed and a practical solution has been found and can be used in tandem with the IDT colour transfer.

It is important to realise that one-to-one colour transfer techniques are not the universal answer to colour grading. The methods are indeed limited by the ability of one-to-one mapping to model change of colour grade. Also, these methods assume that the target image contains the exact colour distribution. In practice however, target images are only an approximation of the desired colour palette. Dealing with content variations is still an open problem, even though some pre and post processing can improve the robustness.

The problems and techniques methods discussed in this chapter can be viewed as a set of tools that one can use confidently, provided that their conditions of use are well understood.



(a1) at evening



(b1) with clouds



(a2) at sunset



(b2) without clouds



(a3) result



(b3) result

Figure 1.12: Examples of colour grading for matching lighting conditions. On the left column, the colour properties of the sunset are used to synthesise the ‘evening’ scene depicted at sunset. On the right column, the colour grading corrects the change of lighting conditions induced by clouds. The colour transfer is achieved by employing IDT followed by the re-graining process.



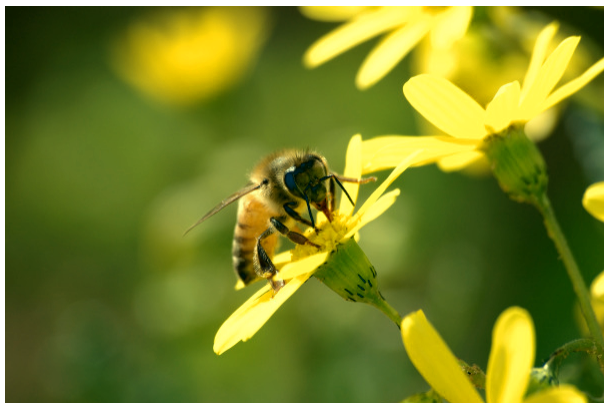
Figure 1.13: Example of colour grading for image and video restoration. It is possible to recreate different atmospheres. Here an old faded film (a) is transformed to match the colour scheme of a movie from the 70's (b) and a pub ambiance (c). The IDT process is followed by the re-graining process.



(a) Original



(b) Target



(c) Linear MK result



(d) IDT result

Figure 1.14: Colour grading results.



Figure 1.15: Colour grading results. The transfer in (c) is done via the Linear MK method and the result in (d) via IDT followed by the re-graining process. The IDT better transfers colour contrasts.

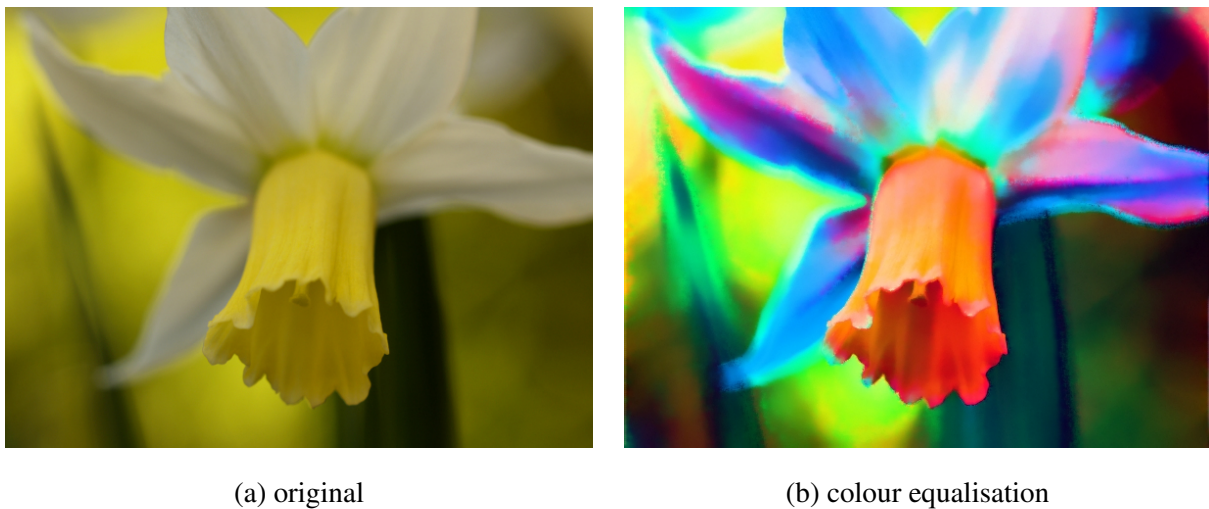


Figure 1.16: Colour Equalisation. The original image (a) is recoloured with the whole colour spectrum using the IDT algorithm followed by the re-graining process.

## Acknowledgement

The authors would like to acknowledge the helpful discussions with the people at The Foundry and Green-ParrotPictures as well as Dr. Naomi Harte for her precious help.

# Bibliography

- [1] M. Pappas and I. Pitas, “Digital Color Restoration of Old Paintings,” *Transactions on Image Processing*, vol. 9, pp. 291–294, February 2000.
- [2] L. Lucchese and S. K. Mitra, “A new Method for Color Image Equalization,” in *Proceedings of the IEEE International Conference on Image Processing (ICIP’01)*, vol. 1, (Thessaloniki, Greece), pp. 133–136, October 7-10 2001.
- [3] E. Pichon, M. Niethammer, and G. Sapiro, “Color histogram equalization through mesh deformation,” in *IEEE International Conference on Image Processing (ICIP’03)*, vol. 3, (Barcelona, Spain), pp. II 117–120, September 14-17 2003.
- [4] R. Fattal, D. Lischinski, and M. Werman, “Gradient domain high dynamic range compression,” in *Proceedings of the 29th annual conference on Computer graphics and interactive techniques*, (New York, NY, USA), pp. 249–256, ACM Press, July 2002.
- [5] P. Debevec, E. Reinhard, G. Ward, and S. Pattanaik, “High dynamic range imaging,” in *ACM SIGGRAPH 2004 Course Notes*, (New York, NY, USA), p. 14, ACM Press, 2004.
- [6] T. Welsh, M. Ashikhmin, and K. Mueller, “Transferring color to greyscale images,” *ACM Transactions on Graphics (Proceedings of ACM SIGGRAPH 2002)*, vol. 21, no. 3, pp. 277–280, 2002.
- [7] Y. Ji, H.-B. Liu, X.-K. Wang, and Y.-Y. Tang, “Color Transfer to Greyscale Images using Texture Spectrum,” in *Proceedings of the Third International Conference on Machine Learning and Cybernetics*, vol. 7, (Shanghai, China), pp. 4057–4061, August 26-29 2004.
- [8] A. A. Gooch, S. C. Olsen, J. Tumblin, and B. Gooch, “Color2gray: salience-preserving color removal,” *ACM Transactions on Graphics (Proceedings of ACM SIGGRAPH 2005)*, pp. 634–639, 2005.
- [9] E. Reinhard, M. Ashikhmin, B. Gooch, and P. Shirley, “Color transfer between images,” *IEEE Computer Graphics Applications*, vol. 21, no. 5, pp. 34–41, 2001.
- [10] A. Abadpour and S. Kasaei, “A fast and efficient fuzzy color transfer method,” in *Proceedings of the IEEE Symposium on Signal Processing and Information Technology*, (Rome, Italy), pp. 491–494, December 18-21 2004.

- [11] L. Neumann and A. Neumann, “Color style transfer techniques using hue, lightness and saturation histogram matching,” in *Proceedings of Computational Aesthetics in Graphics, Visualization and Imaging*, pp. 111–122, May 2005.
- [12] C. M. Wang and Y. H. Huang, “A novel color transfer algorithm for image sequences,” *Journal of Information Science and Engineering*, vol. 20, pp. 1039–1056, November 2004.
- [13] F. Pitié, A. Kokaram, and R. Dahyot, “N-Dimensional Probability Density Function Transfer and its Application to Colour Transfer,” in *International Conference on Computer Vision (ICCV'05)*, (Beijing, China), October 2005.
- [14] H. L. Shen and J. H. Xin, “Transferring color between three-dimensional objects,” *Applied Optics*, vol. 44, pp. 1969–1976, April 2005.
- [15] A. Efros and T. K. Leung, “Texture synthesis by non-parametric sampling,” in *Proceedings of the IEEE International Conference on Computer Vision (ICCV'99)*, (Corfu, Greece), pp. 1033–1038, September 1999.
- [16] A. A. Efros and W. T. Freeman, “Image quilting for texture synthesis and transfer,” in *SIGGRAPH '01: Proceedings of the 28th annual conference on Computer graphics and interactive techniques*, (New York, NY, USA), pp. 341–346, ACM, 2001.
- [17] A. Hertzmann, C. E. Jacobs, N. Oliver, B. Curless, and D. H. Salesin, “Image analogies,” in *SIGGRAPH '01: Proceedings of the 28th annual conference on Computer graphics and interactive techniques*, (New York, NY, USA), pp. 327–340, ACM, 2001.
- [18] S. Bae, S. Paris, and F. Durand, “Two-scale tone management for photographic look,” *ACM Transactions on Graphics (Proceedings of ACM SIGGRAPH 2006)*, pp. 637–645, 2006.
- [19] H. Kotera, “A scene-referred color transfer for pleasant imaging on display,” in *Proceedings of the IEEE International Conference on Image Processing*, (Genoa, Italy), pp. 5–8, September 11-12 2005.
- [20] J. Morovic and P.-L. Sun, “Accurate 3d image colour histogram transformation,” *Pattern Recognition Letters*, vol. 24, pp. 1725–1735, July 2003.
- [21] L. C. Evans, “Partial differential equations and monge-kantorovich mass transfer,” *Current Developments in Mathematics*, 1997, pp. 65–126, 1998.
- [22] W. Gangbo and R. McCann, “The geometry of optimal transport,” *Acta Mathematica*, vol. 177, pp. 113–161, 1996.
- [23] C. Villani, *Topics in Optimal Transportation*, vol. 58 of *Graduate Studies in Mathematics*. Providence, RI: American Mathematical Society, 2003.
- [24] J. Jia, J. Sun, C.-K. Tang, and H.-Y. Shum, “Bayesian correction of image intensity with spatial consideration,” in *Proceedings of the 8th European Conference on Computer Vision (ECCV'04)*, pp. 342–354, May 2004.
- [25] Y. Chang, S. Saito, K. Uchikawa, and M. Nakajima, “Example-based color stylization of images,” *ACM Transactions on Applied Perception*, vol. 2, no. 3, pp. 322–345, 2005.

- [26] R. Lukac, B. Smolka, K. Martin, K. N. Plataniotis, and A. N. Venetsanopoulos, “Vector filtering for color imaging,” *IEEE Signal Processing Magazine*, vol. 22, pp. 74–86, January 2005.
- [27] R. Lukac and K. N. Plataniotis, “A taxonomy of color image filtering and enhancement solutions,” *Advances in Imaging and Electron Physics*, vol. 140, pp. 187–264, June 2006.
- [28] P. Pérez, A. Blake, and M. Gangnet, “Poisson image editing,” *ACM Transactions on Graphics (SIGGRAPH’03)*, vol. 22, pp. 313–318, August 2003.
- [29] B. W. Silverman, *Density Estimation for Statistics and Data Analysis*. Chapman and Hall, 1986.
- [30] R. C. Gonzalez and R. E. Woods, *Digital Image Processing*. Addison Wesley, 1992.
- [31] E. Reinhard, M. Stark, P. Shirley, and J. Ferwerda, “Photographic tone reproduction for digital images,” *ACM Transactions on Graphics (Proceedings of ACM SIGGRAPH 2002)*, vol. 21, no. 3, pp. 267–276, 2002.
- [32] D. L. Ruderman, T. W. Cronin, and C. C. Chiao, “Statistics of Cone Responses to Natural Images: Implications for Visual Coding,” *Journal of the Optical Society of America*, vol. 15, no. 8, pp. 2036–2045, 1998.
- [33] F. Pitié, *Statistical Signal Processing Techniques for Visual Post-Production*. PhD thesis, University of Dublin, Trinity College, April 2006.
- [34] A. Abadpour and S. Kasaei, “An efficient pca-based color transfer method,” *Journal of Visual Communication and Image Representation*, vol. 18, no. 1, pp. 15–34, 2007.
- [35] H. J. Trussell and M. J. Vrhel, “Color correction using principle components,” in *Proceedings of the Society of Photo-Optical Instrumentation Engineers (SPIE)* (M. R. Civanlar, S. K. Mitra, and R. J. Moorhead, II, eds.), vol. 1452, pp. 2–9, June 1991.
- [36] I. Olkin and F. Pukelsheim, “The distance between two random vectors with given dispersion matrices,” *Linear Algebra and its Applications*, vol. 48, pp. 257–263, 1982.
- [37] M. Grundland and N. A. Dodgson, “Color histogram specification by histogram warping,” in *Proceedings of the SPIE Color Imaging X: Processing, Hardcopy, and Applications*, vol. 5667, pp. 610–624, January 2005.
- [38] Y. Rubner, C. Tomasi, and L. J. Guibas, “The earth mover’s distance as a metric for image retrieval,” *International Journal Computer Vision*, vol. 40, pp. 99–121, November 2000.
- [39] F. L. Hitchcock, “The distribution of a product from several sources to numerous localities,” *Journal of Mathematical Physics*, vol. 20, pp. 224–230, 1941.
- [40] N. Wu and R. Coppins, *Linear Programming and Extensions*. New York: McGraw-Hill, 1981.
- [41] F. Pitié, A. Kokaram, and R. Dahyot, “Automated colour grading using colour distribution transfer,” *Journal of Computer Vision and Image Understanding*, February 2007.
- [42] S. Helgason, *The Radon Transform, 2nd edition*. Birkhäuser, 1999.
- [43] J. Weickert, B. ter Haar Romeny, and M. Viergever, “Efficient and reliable schemes for nonlinear diffusion filtering,” *IEEE Transactions on Image Processing*, vol. 7, pp. 398–410, March 1998.

- [44] W. Press, S. Teukolsky, W. Vetterling, and B. Flannery, *Numerical Recipes in C: The Art of Scientific Computing*. New York, NY, USA: Cambridge University Press, 1992.
- [45] F. Pitié, R. Dahyot, F. Kelly, and A. C. Kokaram, “A new robust technique for stabilizing brightness fluctuations,” in *2nd Workshop on Statistical Methods in Video Processing*, (Prague, Czech Republic), May 2004.

# Index

Cholesky Decomposition, 9  
Colour Balancing, 2  
Colour Equalisation, 27  
Colour Grading, 2  
Colour Space  
 $l\alpha\beta$ , 9  
Colour Transfer, 2  
  
Earth Mover Distance, 12  
  
Grading, 2  
  
High Dynamic Range Compression, 21  
  
Iterative Distribution Transfer Algorithm, 14  
  
Kantorovitch's Problem, 7  
  
Mass Transportation Problem, 6  
Monge's Problem, 7  
Movie Restoration, 24  
  
Poisson Image Editing, 21  
Post-Production, 2  
Principal Component Analysis, 10  
Probability Density Estimation, 6  
  
Radon Transform, 12